

Novel probes establish MrgprX1 variants as receptors with loss or gain of function

Daniel Heller, Jamie R. Doyle, Venkata S. Raman, Martin Beinborn, Krishna Kumar, and Alan S. Kopin

Author Affiliations:

Tufts Medical Center, Molecular Cardiology Research Institute, Molecular Pharmacology Research Center, 800 Washington St., Box 7703, Boston, MA 02111 (DH, JRD, MB, and ASK)

Tufts University, Department of Chemistry, 62 Talbot Ave, Medford, MA 02155 (VSR and KK)

Running Title: *Novel probes establish LOF and GOF MrgprX1 variants*

Corresponding Author:

Alan S. Kopin
800 Washington Street, P.O. Box 7703,
Boston, MA, 02111, USA.
Tel.: +1 617-636-4834, Fax: +1 617-636-8692
E-mail: akopin@tuftsmedicalcenter.org

Manuscript Information:

Number of text pages: 14
Number of tables: 3
Number of figures: 7
Number of references: 34
Number of words in Abstract: 191
Number of words in Introduction: 528
Number of words in Discussion: 816

Abbreviations:

GPCR, G protein-coupled receptor; DRG, Dorsal root ganglion; BAM8-22, Bovine Adrenal Medulla peptide 8-22; γ 2-MSH, γ 2-melanocyte stimulating hormone; SNP, single nucleotide polymorphism; MTL, Membrane Tethered Ligand; SMAL, Synthetic Membrane Anchored Ligand; HA, hemagglutinin; HEK293, human embryonic kidney 293; DMEM, Dulbecco's modified Eagle's medium; CMV, cytomegalovirus promoter; ONPG, 2-nitrophenyl β -D-galactopyranoside; HRP, horseradish peroxidase; ELISA, enzyme-linked immunosorbent assay; hMOR, human μ -opioid receptor

Recommended section assignment: Cellular and Molecular

Abstract

The Mas-related G protein-coupled receptor X1 (MrgprX1) is a human seven transmembrane-domain protein with a putative role in nociception and pruritus. This receptor is expressed in dorsal root ganglion (DRG) neurons and is activated by a variety of endogenous peptides, including bovine adrenal medulla peptide (BAM) and γ -melanocyte stimulating hormone (γ 2-MSH). In the present work, we study how naturally occurring missense mutations alter the activity of MrgprX1. To characterize selected receptor variants, we initially used the endogenous peptide ligand BAM8-22. In addition, we generated and characterized a panel of novel recombinant and synthetic peptide ligands. Our studies identified a mutation in the second intracellular loop of MrgprX1, R131S, that causes a decrease in both ligand-mediated and constitutive signaling. Another mutation in this region, H133R, results in a gain of function phenotype reflected by an increase in ligand-mediated signaling. Using epitope-tagged variants, we determined that the alterations in basal and ligand-mediated signaling were not explained by changes in receptor expression levels. Our results demonstrate that naturally occurring mutations can alter the pharmacology of MrgprX1. This study provides a theoretical basis for exploring whether MrgprX1 variability underlies differences in somatosensation within human populations.

Introduction

The Mas-related G protein-coupled receptor X1 (MrgprX1) is a human GPCR expressed in dorsal root ganglia (DRG) neurons (Dong et al., 2001; Lembo et al., 2002). The endogenous ligands bovine adrenal medulla peptide 8-22 (BAM8-22) and γ 2-MSH activate this receptor and trigger $G\alpha_q$ mediated signaling (Lembo et al., 2002; Solinski et al., 2014; Tatemoto et al., 2006). Existing literature suggests that in mouse models, receptors in the Mrgpr family modulate nociception and pruriception *in vivo* (Guan et al., 2010; Liu et al., 2009; Solinski et al., 2014). A recent report showed that in humans, BAM8-22 produces itching sensations through a histamine-independent pathway (Sikand et al., 2011). Despite these studies, there still remain many unanswered questions regarding the precise role of MrgprX1 in mediating somatosensory signals. Analysis of the coding region of the MrgprX1 gene has revealed genetic variation among humans (NHLBI GO Exome Sequencing Project), outlined in Figure 1A and Table 1. To our knowledge, however, the potential impact of naturally occurring missense mutations on the pharmacological properties of MrgprX1 has not yet been studied.

In the past, naturally occurring variants of GPCRs have proved helpful in understanding differences in susceptibility to disease. For example, loss of function mutations in the melanocortin 4 receptor may account for up to 6% of individuals with severe, early-onset obesity (Loos, 2011). Additionally, polymorphisms in chemokine receptors CCR5 and CCR2 have been linked to delayed progression of AIDS after HIV infection (Reiche et al., 2007). Additionally, changes in chemosensory response to sweet and savory tastes are associated with single nucleotide polymorphisms (SNPs) in the GPCRs TAS1R1 and TAS1R3 (Hayes et al., 2013). In an era where genetic information is becoming more accessible to patients and physicians, the link between functional abnormalities in gene products (MrgprX1) and clinical conditions

(pruritus and nociception) can be more readily explored. As an initial step, we have examined the extent to which MrgprX1 missense mutations alter the pharmacological response to the endogenous ligand BAM8-22.

To enable more detailed characterization of signaling differences among MrgprX1 variants, we developed a series of novel agonists (Figure 1B). Previous work in our laboratory has shown that peptide ligands may be anchored to the cell surface using recombinant DNA technology. Such membrane-tethered ligands (MTLs) provide a complementary tool to explore GPCR function (Fortin et al., 2011, 2009; Harwood et al., 2013). Conversion of these recombinant ligands into synthetic membrane anchored ligands (SMALs), in which a peptide is covalently coupled to a flexible linker and a lipid moiety, yields potent, soluble ligands that anchor to the cell surface and activate the corresponding GPCR (Doyle et al., 2014; Fortin et al., 2011). Potential advantages of such ligands include increased potency and prolonged stability (Zhang and Bulaj, 2012).

In the current study, we use this expanded panel of ligands to characterize a series of MrgprX1 missense mutations with an allele frequency exceeding 0.1% (Table 1). A cartoon of MrgprX1 (Figure 1A) highlights the location of each variant residue. We demonstrate that two mutations in MrgprX1, R131S and H133R, alter receptor mediated signaling, resulting in loss and gain of function respectively. We propose that these variants should be assessed in human populations to determine whether they modify susceptibility to histamine-independent itch and/or nociception.

Materials and Methods

Generation of Receptor cDNA Constructs

The MrgprX1 cDNA, in pcDNA 3.1, was generously provided by Dr. Xinzhong Dong (Johns Hopkins University School of Medicine, Baltimore, MD). The construct was subcloned into pcDNA1.1 (Invitrogen). Naturally occurring missense mutations were chosen using data from the NHLBI GO ESP Exome Variant Server [Exome Variant Server, NHLBI Exome Sequencing Project (ESP), Seattle, WA (URL: <http://evs.gs.washington.edu/EVS/>)]. Oligonucleotide-directed site-specific mutagenesis (as in Doyle et al., 2013; Fortin et al., 2009) was used to generate the receptor variants and corresponding epitope-tagged versions (where a hemagglutinin (HA) epitope tag was inserted immediately following the initiator methionine). Forward and reverse DNA sequencing confirmed the correct nucleotide sequences for each construct.

Generation of recombinant Membrane Tethered Ligands (MTLs)

A Membrane Tethered Ligand (MTL) is a cDNA-encoded protein consisting of a peptide ligand fused to a transmembrane domain via a flexible linker region. Type I MTLs include a type I transmembrane domain, which orients the construct such that the N terminus of the ligand is extracellular. Conversely, type II MTLs result in an extracellular C terminus (Chou and Elrod, 1999; Harwood et al., 2013). Corresponding DNA templates were used from previously published tethered exendin (type I) and tethered chemerin (type II) constructs (Doyle et al., 2014; Fortin et al., 2009). DNA sequences corresponding to the peptide ligands were each sequentially replaced with those encoding BAM8-22 (VGRPEWWMDYQKRYG) and γ 2-MSH (YVMGHFRWDRFG) (Lembo et al., 2002) using oligonucleotide-directed site-specific

mutagenesis, producing both type I and type II MTLs for each peptide (Fortin et al., 2009; Harwood et al., 2013).

Generation of Synthetic Membrane Anchored Ligands (SMAL) Constructs

Reagents for peptide synthesis were purchased from Chem-Impex (Wood Dale, IL). N-Fmoc-PEG8-propionic acid, and palmitic acid were obtained from AAPPTec (Louisville, KY) and Sigma-Aldrich (St. Louis, MO) respectively. Peptides were assembled on 4-hydroxymethyl phenylacetamidomethyl (PAM) resin using the insitu neutralization protocol for N-Boc chemistry with 2-(1H-benzotriazol-1-yl)-1,1,3,3-tetramethyluronium hexafluorophosphate (HBTU) as the activating agent on a 0.25 mmol scale (Schnölzer et al., 2007). Peptide coupling reactions were carried out with a 4-fold excess of the protected amino acid (1 mmol). A GGK peptide spacer was added to the C terminus of BAM8-22 to enable coupling of the PEG8 linker.

After completion of the desired peptide sequence, coupling of N-Fmoc-PEG8-propionic acid to the N terminus (γ 2-MSH) or the C terminus (BAM8-22) preceded coupling of the lipid (palmitic acid) using standard activation procedures (Doyle et al., 2014). Peptides were cleaved from the resin by using high HF conditions (90% anhydrous HF/10% anisole at 0 °C for 1.5 h), and precipitated using cold Et₂O. Crude peptides were purified by reversed phase HPLC, and the purities determined by analytical HPLC [Vydac, C18, 5 μ , 4 mm \times 250 mm] with a linear gradient of solvent B over 20 mins at a flow rate of 1 mL/min. Elution was monitored by absorbance at 230 nm. Purities of peptides ranged from 90-95%. Peptides were analytically characterized by MALDI-TOF mass spectrometry.

MarvinSketch was used for drawing and displaying chemical structures (Table 2); MarvinSketch v14.9.1, 2014, ChemAxon (<http://www.chemaxon.com>).

Transfection and Luciferase Reporter Gene Assay

A luciferase reporter-based assay was utilized as an index of receptor-mediated signaling (as in Doyle et al., 2013). Human kidney cells (HEK293), grown in Dulbecco's modified Eagle's medium (DMEM) containing 10% FBS, 100 U/ml penicillin, and 100 µg/ml streptomycin were seeded in 96-well plates and grown to 80% confluence. Using polyethylenimine (PEI, 2.0 µg/mL in serum-free DMEM), cells were transiently transfected with cDNAs encoding (a) wild type or variant MrgprX1 (3 ng/well); (b) an SRE-luciferase PEST construct (SRE_{5x}-Luc-PEST), which includes five SRE repeats, a luciferase reporter gene, and the protein degradation sequence hPEST (Promega, catalog #E1340) (25 ng/well); and (c) a CMV-β-galactosidase construct as a control for variability in transfection efficiency (10 ng/well). In experiments that included transfection of an MTL-encoding construct, the corresponding cDNA was added to the transfection mix, at 4 ng/well or as indicated.

Twenty-four hours following transfection, cells were stimulated with soluble ligand for 4 hours (if applicable). After addition of SteadyLite reagent (PerkinElmer, Chicago, IL.), luciferase activity of the lysate was measured using a TopCount NTX plate reader. Subsequently, 2-nitrophenyl β-D-galactopyranoside (ONPG) was added as a colorimetric substrate to enable quantification of β-galactosidase levels. After incubation with ONPG for 30 minutes, absorbance at 420 nm was measured using a SpectraMax microplate reader (Molecular Devices). Luciferase activity was normalized using the β-galactosidase activity data. Three independent experiments were performed, each with three technical replicates. Data were graphed and statistically analyzed using Graphpad Prism software.

Enzyme-Linked Immunosorbent Assay (ELISA)

An ELISA was used to assess total and surface receptor expression (as in Doyle et al., 2013). In brief, HEK293 cells were grown and seeded as above using 96-well plates pretreated

with poly-L-lysine. When 80% confluent, cells were transfected with HA-tagged receptor constructs. After 24 hours, the cells were fixed with 4% paraformaldehyde in phosphate buffered saline (PBS) for 10 min. To measure total expression levels, 0.1% Triton X-100 in PBS was applied in order to permeabilize the cell membrane. To assess surface expression, treatment with Triton X-100 was omitted. Cells were washed with PBS/100 mM glycine and then incubated in PBS/20% FBS for 30 minutes in order to block nonspecific antibody binding. A horseradish peroxidase (HRP)-conjugated antibody directed against the HA epitope tag (Roche, catalog #12013819001) was diluted 1:500 and added to the cells for 3 hours. Cells were then washed 5 times with PBS. The HRP substrate BM-blue (3,3'-5,5'-tetramethylbenzidine, Roche) was added at 50 μ l per well. After 30 minutes, 50 μ l of 2.0 M sulfuric acid was added to each well to stop the reaction. The concentration of the colorimetric product was quantified by measuring absorbance at 450nm using a SpectraMax microplate reader (Molecular Devices).

Data Analysis

GraphPad Prism software version 6.0 (GraphPad Software Inc., La Jolla, CA) was used for sigmoidal curve fitting of ligand concentration–response curves, linear regression, and statistical analysis. EC_{50} and pEC_{50} values were calculated for each independent experiment as an index of ligand potency. Reported values represent the mean of three independent experiments. Statistical comparisons were made by one-way analysis of variance with Dunnett's multiple comparisons test.

Results

Missense mutations in MrgprX1 result in differing levels of endogenous peptide-mediated signaling.

Signaling of MrgprX1 following stimulation with the endogenous peptide ligand BAM8-22 was measured using a luciferase reporter assay as described in Methods. Cells expressing MrgprX1 (WT or variant receptors) were stimulated for 4 hours with soluble BAM8-22. Concentration-response curves presented in Figure 2 illustrate that six of the seven MrgprX1 variants assayed have a normal response to the ligand. However, the R131S variant exhibited lower levels of BAM8-22 mediated activity. The R131S best-fit curve is shifted to the right, suggesting a significant loss of potency. Since soluble BAM8-22 does not fully stimulate the receptors when applied at the highest tested concentration (10 μ M), accurate EC₅₀ values could not be calculated. It should be noted that HEK293 cells transfected with an empty vector control show no activity after treatment with ligand (data not shown).

Characterization of novel recombinant and synthetic MrgprX1 ligands.

As additional tools for structure-function studies, MTLs incorporating one of two endogenous peptide ligands for MrgprX1, BAM8-22 and γ 2-MSH, were generated. The activities of MTL constructs in both orientations (type I, with an extracellular N terminus of the ligand; type II, with an extracellular C terminus) were assessed using a luciferase-based reporter assay as described in Methods. When expressed in HEK293 cells together with MrgprX1, a subset of MTL constructs activated the receptor in a cDNA concentration-dependent manner (Figure 3A, 3B). Active MTLs included type I tethered BAM8-22 (free extracellular N terminus) and type II tethered γ 2-MSH (free extracellular C terminus). These constructs were therefore used in subsequent experiments.

Previous studies have shown that the activity of recombinant MTLs can be recapitulated using synthetic membrane anchored ligands (SMALs) which integrate into the cellular membrane via a lipid moiety (Doyle et al., 2014; Fortin et al., 2011). Lipidated constructs were generated corresponding to the two active MrgprX1 MTLs. Guided by the MTL results, PEG8 and palmitic acid were covalently attached to the C-terminus of BAM8-22 and the N terminus of γ 2-MSH to generate corresponding SMALs (Table 2). When compared to the endogenous soluble form, both lipidated BAM8-22 and lipidated γ 2-MSH displayed significantly increased potency (Figure 3C, 3D).

In a parallel set of experiments (data not shown), signaling levels at saturating concentrations of the four novel MrgprX1 ligands were assessed at the WT receptor. Tethered BAM8-22, tethered γ 2-MSH, and lipidated γ 2-MSH signaling represented 38.4 ± 5.4 , 12.9 ± 2.0 , and $67.9\% \pm 2.4$ (mean \pm SEM) of maximum lipidated BAM8-22 signaling (at 10^{-7} M), respectively.

Select MrgprX1 missense mutations result in altered ligand mediated signaling.

The activity of tethered and lipidated BAM8-22 at each of the seven MrgprX1 variants was assessed (Figure 4). Following stimulation with either the recombinant or the synthetic BAM8-22 analog, the R131S variant consistently displays attenuated levels of signaling. In addition to decreased efficacy, a statistical analysis of calculated EC_{50} values for all seven variants suggests that only the R131S mutation significantly decreases the potency and efficacy of lipidated BAM8-22 (Table 3).

The R131S variant also displays decreased ligand-mediated signaling with either tethered or lipidated γ 2-MSH (Figure 5). Additionally, the H133R mutation significantly increases tethered and lipidated γ 2-MSH mediated signaling, an effect not observed with lipidated or

tethered BAM8-22. A moderate decrease in signaling with the R55L and F273L variants was observed with both tethered BAM8-22 and tethered γ 2-MSH, although this decrease only reached statistical significance with tethered γ 2-MSH.

The R131S missense mutation reduces the basal activity of MrgprX1.

To explore whether changes in receptor-mediated signaling levels in part reflect altered basal activity, ligand-independent signaling of the R131S and the H133R variants was assessed (Figure 6). Wild type MrgprX1 exhibits significant basal activity approximating 6% of the maximum BAM8-22 stimulated level of signaling (at 10 μ M). The H133R variant shows basal activity levels comparable to WT. In contrast, the R131S variant shows markedly attenuated ligand-independent activity.

Expression levels of the R131S and H133R variants are comparable to wild type.

We next explored the possibility that the observed differences in ligand-dependent and ligand-independent signaling were the result of altered receptor expression. An enzyme-linked immunosorbent assay (ELISA) was used for this analysis. We generated epitope-tagged versions of WT MrgprX1, and of the R131S and H133R variants. Each receptor was expressed in HEK293 cells. Both the R131S and H133R variants exhibit levels of total and surface expression comparable to WT MrgprX1 (Figure 7). These data suggest that observed differences in signaling are not attributable to changes in receptor expression.

Discussion

Initial analysis of naturally occurring MrgprX1 variants with the endogenous ligand BAM8-22 identified R131S as a potential loss-of-function mutation (Figure 2). To further investigate ligand-mediated signaling of this variant as well as other receptor mutants, MTL and SMAL analogs of BAM8-22 and γ 2-MSH were generated. In addition to confirming the loss of function resulting from the R131S mutation, use of these recombinant and synthetic ligands revealed that the H133R substitution conferred a ligand-dependent gain of function phenotype (Figures 4 and 5). Defining how missense mutations in this receptor alter pharmacological function is an important first step towards understanding the potential role of natural variants in altering somatosensation and/or the response to drugs targeting MrgprX1 *in vivo*.

There are multiple mechanisms through which missense mutations may affect GPCR function. Some variants affect the active/inactive state equilibrium and may in turn have systematic effects on ligand-mediated signaling (Beinborn et al., 2004; Kopin et al., 2003; Samama et al., 1993). Other mutations alter ligand interaction with the receptor, either directly or indirectly through changes in receptor tertiary structure. (Bond et al., 1998; Fortin et al., 2010).

Data presented in this report suggests that the R131S mutation decreases both ligand-mediated and ligand-independent (basal) activity of MrgprX1. These properties place it in the former group of mutations. Notably, these differences in receptor activity levels cannot be explained by changes in receptor expression (Figure 7). The location of residue R131 in the second intracellular loop, a domain that has been established as important in G protein binding (Hu et al., 2010), suggests that this mutation could be affecting the ability of MrgprX1 to interact with G proteins and/or shift MrgprX1 from the active to the inactive state.

The H133R mutation does not affect basal activity and slightly increases the efficacy of a subset of ligands (i.e. tethered and lipidated γ 2-MSH but not tethered or lipidated BAM8-22). This suggests that H133R is not a systematic modulator and therefore belongs to the latter group of mutations (as described above). Like with R131S, these changes in ligand-mediated receptor activity are not accompanied by changes in receptor expression. Given its location in the second intracellular loop, H133R may represent a mutation that impacts the ligand-receptor interaction indirectly (e.g. by slightly altering the orientation of residues that interact with the ligand).

The purported role of MrgprX1 in mediating pain and somatosensation, in particular histamine-independent itch (Bader et al., 2014; Sikand et al., 2011; Solinski et al., 2014), suggests that the unique signaling properties of the R131S and H133R variants may have important implications for the development and use of therapeutics targeting this receptor. Missense variants have also proven important in understanding differences in somatosensation in the past. For example, the N40D mutation in the human μ -opioid receptor (hMOR) may alter susceptibility to pain (Lötsch and Geisslinger, 2005) and pruritus (Tsai et al., 2010). Similarly, missense mutations in the sodium channel $Na_v1.7$ have been linked to pain-related disorders (Drenth and Waxman, 2007; Fertleman et al., 2006) and altered pain perception (Reimann et al., 2010).

The possibility that MrgprX1 variants may be linked to a specific phenotype highlights the need for data collection that will allow for matching of the MrgprX1 genotype with sensitivity to MrgprX1-mediated somatosensation. This should be feasible particularly with the R131S variant, which has an allele frequency of greater than 1%. Future studies may reveal that mutations such as R131S are linked to decreased nociception or pruritus. Extending beyond the coding region of the gene, variations in upstream regulatory sequences may also play a role in

altering susceptibility to histamine-independent itch by altering MrgprX1 expression (Wray, 2007).

Although mutational analysis with the naturally occurring agonist-receptor pair is most physiologically relevant, MTLs and their lipidated counterparts can provide powerful molecular probes to explore pharmacological differences between receptor variants. As illustrated, such modified peptide ligands exhibit enhanced effective concentration and thus provide experimental tools that facilitate the pharmacological characterization of GPCRs. In addition, MTLs can be expressed as transgenic constructs enabling exploration of corresponding receptor function *in vivo* (Harwood et al., 2014). Complementing such recombinant constructs, lipidated peptides provide additional tools which can be applied *in vivo* to probe receptor function and validate potential therapeutic targets (Doyle et al., 2014). Notably, activity of tethered γ 2-MSH and tethered BAM8-22 are recapitulated with their lipidated analogs, providing further support that MTLs may be useful in predicting the pharmacological properties of corresponding lipidated peptides.

Taken together, our experiments illustrate how naturally occurring missense variants may markedly alter the pharmacological properties of a GPCR. In addition, our data exemplify how MTLs and SMALs provide complementary tools to differentiate receptor variants that are systematic modulators from mutations that preferentially affect a subset of receptor agonists. As with a growing number of GPCRs (Rana et al., 2001; Thompson et al., 2014), MrgprX1 receptor variants display important differences in both basal and ligand-induced signaling that may contribute to somatosensory variability in the human population.

Acknowledgements

The authors would like to thank Ci Chen (Tufts Medical Center) for technical assistance, as well as Ben Harwood, Bina Julian, and Isabelle Draper (Tufts Medical Center) for invaluable advice and support.

The NHLBI GO Exome Sequencing Project and its ongoing studies produced and provided exome variant calls for comparison: the Lung GO Sequencing Project (HL-102923), the WHI Sequencing Project (HL-102924), the Broad GO Sequencing Project (HL-102925), the Seattle GO Sequencing Project (HL-102926) and the Heart GO Sequencing Project (HL-103010).

Authorship Contributions

Participated in research design: Heller, Doyle, Raman, Kumar, Kopin.

Conducted experiments: Heller, Doyle.

Contributed new reagents or analytic tools: Raman, Kumar.

Performed data analysis: Heller.

Wrote or contributed to the writing of the manuscript: Heller, Doyle, Beinborn, Raman,
Kumar, Kopin.

References

- Bader M, Alenina N, Andrade-Navarro MA, and Santos RA (2014) Mas and Its Related G Protein-Coupled Receptors, Mrgprs. *Pharmacol Rev* **66**:1080–1105.
- Beinborn M, Ren Y, Bläker M, Chen C, and Kopin AS (2004) Ligand function at constitutively active receptor mutants is affected by two distinct yet interacting mechanisms. *Mol Pharmacol* **65**:753–60.
- Bond C, LaForge KS, Tian M, Melia D, Zhang S, Borg L, Gong J, Schluger J, Strong JA, Leal SM, Tischfield JA, Kreek MJ, and Yu L (1998) Single-nucleotide polymorphism in the human mu opioid receptor gene alters beta-endorphin binding and activity: possible implications for opiate addiction. *Proc Natl Acad Sci USA* **95**:9608–13.
- Chou KC, and Elrod DW (1999) Prediction of membrane protein types and subcellular locations. *Proteins* **34**:137–53.
- Dong X, Han S, Zylka MJ, Simon MI, and Anderson DJ (2001) A diverse family of GPCRs expressed in specific subsets of nociceptive sensory neurons. *Cell* **106**:619–32.
- Doyle JR, Krishnaji ST, Zhu G, Xu Z-Z, Heller D, Ji R-R, Levy BD, Kumar K, and Kopin AS (2014) Development of a Membrane-anchored Chemerin Receptor Agonist as a Novel Modulator of Allergic Airway Inflammation and Neuropathic Pain. *J Biol Chem* **289**:13385–96.
- Doyle JR, Lane JM, Beinborn M, and Kopin AS (2013) Naturally occurring HCA1 missense mutations result in loss of function: potential impact on lipid deposition. *J Lipid Res* **54**:823–30.
- Drenth JPH, and Waxman SG (2007) Mutations in sodium-channel gene SCN9A cause a spectrum of human genetic pain disorders. *J Clin Invest* **117**:3603–9.
- Fertleman CR, Baker MD, Parker KA, Moffatt S, Elmslie F V, Abrahamsen B, Ostman J, Klugbauer N, Wood JN, Gardiner RM, and Rees M (2006) SCN9A mutations in paroxysmal extreme pain disorder: allelic variants underlie distinct channel defects and phenotypes. *Neuron* **52**:767–74.
- Fortin J-P, Chinnapen D, Beinborn M, Lencer W, and Kopin AS (2011) Discovery of dual-action membrane-anchored modulators of incretin receptors. *PLoS One* **6**:e24693.

- Fortin J-P, Ci L, Schroeder J, Goldstein C, Montefusco MC, Peter I, Reis SE, Huggins GS, Beinborn M, and Kopin AS (2010) The μ -opioid receptor variant N190K is unresponsive to peptide agonists yet can be rescued by small-molecule drugs. *Mol Pharmacol* **78**:837–45.
- Fortin J-P, Zhu Y, Choi C, Beinborn M, Nitabach MN, and Kopin AS (2009) Membrane-tethered ligands are effective probes for exploring class B1 G protein-coupled receptor function. *Proc Natl Acad Sci U S A* **106**:8049–54.
- Guan Y, Liu Q, Tang Z, Raja SN, Anderson DJ, and Dong X (2010) Mas-related G-protein-coupled receptors inhibit pathological pain in mice. *Proc Natl Acad Sci U S A* **107**:15933–8.
- Harwood BN, Draper I, and Kopin AS (2014) Targeted inactivation of the rickets receptor in muscle compromises *Drosophila* viability. *J Exp Biol* **217**:4091–8.
- Harwood BN, Fortin J-P, Gao K, Chen C, Beinborn M, and Kopin AS (2013) Membrane tethered bursicon constructs as heterodimeric modulators of the *Drosophila* G protein-coupled receptor rickets. *Mol Pharmacol* **83**:814–21.
- Hayes JE, Feeney EL, and Allen AL (2013) Do polymorphisms in chemosensory genes matter for human ingestive behavior? *Food Qual Prefer* **30**:202–216.
- Hu J, Wang Y, Zhang X, Lloyd JR, Li JH, Karpiak J, Costanzi S, and Wess J (2010) Structural basis of G protein-coupled receptor-G protein interactions. *Nat Chem Biol* **6**:541–8.
- Kopin AS, McBride EW, Chen C, Freidinger RM, Chen D, Zhao C-M, and Beinborn M (2003) Identification of a series of CCK-2 receptor nonpeptide agonists: sensitivity to stereochemistry and a receptor point mutation. *Proc Natl Acad Sci U S A* **100**:5525–30.
- Lembo PMC, Grazzini E, Groblewski T, O'Donnell D, Roy M-O, Zhang J, Hoffert C, Cao J, Schmidt R, Pelletier M, Labarre M, Gosselin M, Fortin Y, Banville D, Shen SH, Ström P, Payza K, Dray A, Walker P, and Ahmad S (2002) Proenkephalin A gene products activate a new family of sensory neuron--specific GPCRs. *Nat Neurosci* **5**:201–9.

- Liu Q, Tang Z, Surdenikova L, Kim S, Patel KN, Kim A, Ru F, Guan Y, Weng H-J, Geng Y, Udem BJ, Kollarik M, Chen Z-F, Anderson DJ, and Dong X (2009) Sensory neuron-specific GPCR Mrgprs are itch receptors mediating chloroquine-induced pruritus. *Cell* **139**:1353–65.
- Loos RJF (2011) The genetic epidemiology of melanocortin 4 receptor variants. *Eur J Pharmacol* **660**:156–64.
- Lötsch J, and Geisslinger G (2005) Are mu-opioid receptor polymorphisms important for clinical opioid therapy? *Trends Mol Med* **11**:82–9.
- Rana BK, Shiina T, and Insel PA (2001) Genetic variations and polymorphisms of G protein-coupled receptors: functional and therapeutic implications. *Annu Rev Pharmacol Toxicol* **41**:593–624, Annual Reviews 4139 El Camino Way, P.O. Box 10139, Palo Alto, CA 94303-0139, USA.
- Reiche EM V., Bonametti AM, Voltarelli JC, Morimoto HK, and Watanabe MAE (2007) Genetic polymorphisms in the chemokine and chemokine receptors: impact on clinical course and therapy of the human immunodeficiency virus type 1 infection (HIV-1). *Curr Med Chem* **14**:1325–34,
- Reimann F, Cox JJ, Belfer I, Diatchenko L, Zaykin D V, McHale DP, Drenth JPH, Dai F, Wheeler J, Sanders F, Wood L, Wu T-X, Karppinen J, Nikolajsen L, Männikkö M, Max MB, Kiselycznyk C, Poddar M, Te Morsche RHM, Smith S, Gibson D, Kelempisioti A, Maixner W, Gribble FM, and Woods CG (2010) Pain perception is altered by a nucleotide polymorphism in SCN9A. *Proc Natl Acad Sci USA* **107**:5148–53.
- Samama P, Cotecchia S, Costa T, and Lefkowitz R (1993) A mutation-induced activated state of the beta 2-adrenergic receptor. Extending the ternary complex model. *J Biol Chem* **268**:4625–4636.
- Schnölzer M, Alewood P, Jones A, Alewood D, and Kent SBH (2007) In situ neutralization in boc-chemistry solid phase peptide synthesis: Rapid, high yield assembly of difficult sequences. *Int J Pept Res Ther* **13**:31–44.
- Sikand P, Dong X, and LaMotte RH (2011) BAM8-22 peptide produces itch and nociceptive sensations in humans independent of histamine release. *J Neurosci* **31**:7563–7.

- Solinski HJ, Gudermann T, and Breit A (2014) Pharmacology and Signaling of MAS-Related G Protein-Coupled Receptors. *Pharmacol Rev* **66**:570–597.
- Tatemoto K, Nozaki Y, Tsuda R, Konno S, Tomura K, Furuno M, Ogasawara H, Edamura K, Takagi H, Iwamura H, Noguchi M, and Naito T (2006) Immunoglobulin E-independent activation of mast cell is mediated by Mrg receptors. *Biochem Biophys Res Commun* **349**:1322–8.
- Thompson MD, Hendy GN, Percy ME, Bichet DG, and Cole DEC (2014) G protein-coupled receptor mutations and human genetic disease. *Methods Mol Biol* **1175**:153–87.
- Tsai FF, Fan SZ, Yang YM, Chien KL, Su YN, and Chen LK (2010) Human opioid μ -receptor A118G polymorphism may protect against central pruritus by epidural morphine for post-cesarean analgesia. *Acta Anaesthesiol Scand* **54**:1265–1269.
- Wray GA (2007) The evolutionary significance of cis-regulatory mutations. *Nat Rev Genet* **8**:206–16.
- Zhang L, and Bulaj G (2012) Converting peptides into drug leads by lipidation. *Curr Med Chem* **19**:1602–18.

Footnotes

This work was supported in part by a Charles A. King Trust Postdoctoral Research Fellowship (to J.R.D.) and a Robert Gatof Summer Scholars Grant through Tufts University (to D.H.).

Figure Legends

Figure 1 – Schematic of MrprX1 and corresponding membrane anchored ligands. Panel A:

Cartoon of the MrprX1 seven transmembrane domain structure highlighting the positions of MrprX1 missense mutations. The wild type amino acids in positions where sequence variations occur are indicated by the single letter code. Panel B: Representation of an MTL and a SMAL in relation to a GPCR. MTLs are recombinant proteins which include an anchoring transmembrane domain, a flexible linker and an extracellular peptide ligand. SMALs are synthetic compounds comprised of an anchoring lipid moiety, a synthetic linker region, and a peptide ligand.

Figure 2 – The R131S MrprX1 variant shows reduced endogenous ligand mediated signaling.

HEK293 cells were transfected with cDNA encoding either wild type or variant MrprX1, an SRE-luciferase reporter construct, and β -galactosidase. After 24 hours, cells were stimulated with soluble BAM8-22 for 4 hours. Luciferase activity was quantified and normalized relative to β -galactosidase expression. Three independent experiments were performed in triplicate, and data were expressed relative to the wild type receptor signal (maximum stimulation = 100%). Results are shown as the mean \pm SEM.

****, $p < 0.0001$ vs. WT (at 10^{-5} M)

Figure 3 – Anchored ligands as tools to study MrprX1 signaling. Type I tethered BAM8-22 (panel

A) and type II tethered γ 2-MSH (panel B) are active on the WT receptor. Lipidated BAM8-22 and lipidated γ 2-MSH exhibit increased potency compared to the corresponding soluble peptides (panels C and D, respectively). To determine MTL activity, HEK293 cells were transfected with increasing amounts of cDNA encoding either tethered BAM8-22 or tethered γ 2-MSH, as well as a fixed amount of cDNA encoding wild type MrprX1, an SRE-luciferase reporter construct, and β -galactosidase. To determine synthetic membrane anchored ligand activity, similar methodology was utilized with tether cDNA omitted. Twenty-four hours after transfection, the cells were stimulated with lipidated BAM8-22 or

lipidated γ 2-MSH for 4 hours. Luciferase activity was quantified and normalized relative to β -galactosidase expression. Data shown represent at least two independent experiments performed in triplicate. Results were expressed relative to the wild type receptor signal (maximum = 100%) and graphed as mean \pm SEM.

Figure 4 – The R131S variant exhibits decreased response to stimulation with BAM8-22 analogs.

The R131S variant displays negligible signaling levels with tethered BAM8-22 (panel A) as well as reduced signaling with lipidated BAM8-22 (panel B). To measure MTL activity, HEK293 cells were transfected with cDNAs encoding tethered BAM8-22, either wild type or variant MrgprX1, an SRE-luciferase reporter construct, and β -galactosidase. The empty vector, pcDNA1.1, was transfected instead of receptor cDNA as a control. To measure synthetic membrane anchored ligand activity, a similar methodology was utilized with the tether cDNA omitted. Cells were stimulated 24 hours after transfection with lipidated BAM8-22 for four hours. Luciferase activity was quantified and normalized relative to β -galactosidase expression. For each receptor, three independent experiments were performed in triplicate. Data are expressed relative to the maximum signal achieved at the wild type receptor. Results are shown as the mean \pm SEM. *****, $p < 0.0001$ variant receptor vs. WT (at 10^{-6} M in panel B). All variants except R131S are significantly different from pcDNA1.1 ($p < 0.05$).

Figure 5 – The R131S and H133R variants exhibit altered response to γ 2-MSH analogs. When stimulated with tethered (panel A) or lipidated (panel B) γ 2-MSH, the R131S and H133R variants exhibit decreased and increased signaling levels compared to the wild type receptor, respectively. To measure MTL activity, HEK293 cells were transfected with cDNAs encoding tethered γ 2-MSH, either wild type or variant MrgprX1, an SRE-luciferase reporter construct, and β -galactosidase. The empty vector, pcDNA1.1, was transfected instead of receptor cDNA as a control for background signaling. To measure synthetic membrane anchored ligand activity, the tether cDNA was omitted. Cells were stimulated 24

hours after transfection with lipidated γ 2-MSH for four hours. Luciferase activity was quantified and normalized relative to β -galactosidase expression. For each receptor, three independent experiments were performed in triplicate. Data are expressed relative to the maximum signal achieved at the wild type receptor. Results are shown as the mean \pm SEM. *, $p < 0.05$; **, $p < 0.01$; ****, $p < 0.0001$ vs. WT (at 10^{-7} M in panel B). All variants except R131S are significantly different from pcDNA1.1 ($p < 0.05$).

Figure 6 – The MrgprX1 variant R131S exhibits decreased ligand-independent signaling. To

measure constitutive activity, HEK293 cells were transfected with cDNAs encoding the corresponding MrgprX1 variant, an SRE-luciferase reporter construct, and β -galactosidase. After 24 hours, luciferase activity was quantified and normalized relative to β -galactosidase expression. Three independent experiments were performed in triplicate. Data were expressed relative to the maximum signal on wild type MrgprX1 at 3ng of cDNA, achieved by stimulating with 10^{-5} M soluble BAM8-22 for four hours. Results are shown as the mean \pm SEM and lines were fitted with linear regression. ***, $p < 0.001$ (vs. WT, at 8ng cDNA).

Figure 7 – The R131S and H133R variants are expressed at levels comparable to WT. HEK293 cells

were transfected with increasing amounts of cDNA encoding the respective N-terminally HA epitope tagged MrgprX1 variant. After 24 hours, surface (panel A) and total (panel B) expression levels were assessed by ELISA using non-permeabilized and permeabilized cells, respectively. Differences between expression levels of the WT receptor and the R131S and H133R variants are not statistically significant ($p > 0.05$). After subtraction of background signal (no cDNA transfected), data were expressed relative to maximum wild type MrgprX1 expression in permeabilized cells (total expression). Results are shown as the mean \pm SEM and lines were fitted with linear regression.

Tables

Table 1 - Allele frequencies of MgprX1 missense variants. All data were collected from the NHLBI GO ESP Exome Variant Server. Abbreviations: EA, European American; AA, African American.

Variant	dbSNP Reference ID	EA Frequency	AA Frequency
I36V	rs11024885	0.63%	10.17%
A46T	rs78179510	17.69%	19.24%
R55L	rs55954376	0.01%	3.42%
R131S	rs111448117	1.19%	0.23%
H133R	rs140351170	0.33%	0.07%
H137R	rs143702818	0.01%	0.41%
F273L	rs138263314	2.44%	0.53%

Table 2 - Chemical structure of synthesized lipidated peptides.

Peptide	Structure	Molecular Weights (Da)	
		Calculated ^a	Observed ^b
Lipidated BAM8-22 ^c	$\text{H}_2\text{N-VGRPEWWMDYQKRYGGGK-CO}_2\text{H}$	2875.0	2872.7
Lipidated γ 2-MSH ^d	$\text{HN-YVMGHRWDRFG-CO}_2\text{H}$	2231.2	2230.9

^a Calculated molecular weights were estimated using GenScript (Piscataway, NJ).

^b Observed molecular weights were determined by MALDI-TOF MS (Bruker microflex LT) in a positive reflectron mode using α -cyano-4-hydroxy cinnamic acid as the matrix.

^c Lipidated BAM8-22 is comprised of BAM8-22 and a GGK spacer coupled to a PEG8 linker domain and palmitic acid. Note that the linker-lipid modification is on the amino side chain group (N^ε) of the C-terminal lysine.

^d Lipidated γ 2-MSH is comprised of γ 2-MSH coupled to a PEG8 linker domain and palmitic acid. Note that the linker-lipid modification is on the N terminus of the peptide.

Table 3 – Comparison of signaling induced by lipidated BAM8-22 at selected MrgprX1 variants.

Variant	EC ₅₀ (nM)	pEC ₅₀ ^a	Curve Maximum ^{a,b}
WT	12.0	7.92 ± 0.065	101.3% ± 2.7
I36V	9.3	8.03 ± 0.12	108.9% ± 5.4
A46T	9.5	8.02 ± 0.112	111.6% ± 5.2
R55L	10.2	7.99 ± 0.142	107.5% ± 6.4
R131S	57.1	7.24 ± 0.117 ^{****}	40.4% ± 2.5 ^{****}
H133R	8.6	8.06 ± 0.103	110.2% ± 4.6
H137R	7.9	8.10 ± 0.089	109.2% ± 4.0
F273L	12.1	7.92 ± 0.076	95.9% ± 3.1

^a, shown as mean ± SEM

^b, curve maxima are extrapolated from the best-fit curve. Luciferase signal at the WT receptor achieved at 10⁻⁶ M lipidated BAM8-22 is defined as 100%.

^{****}, p<0.0001 (vs. WT)

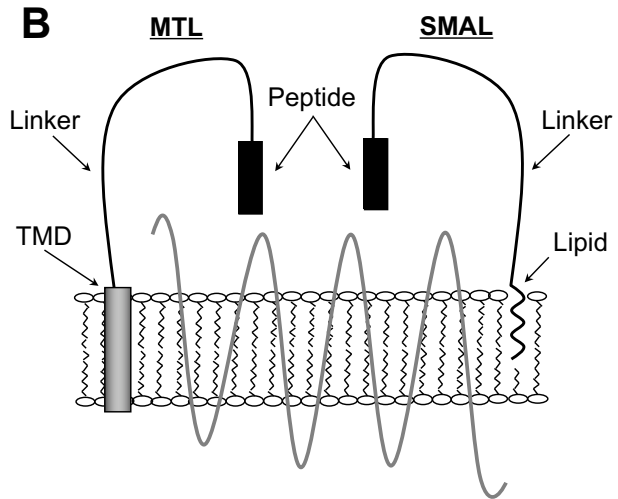
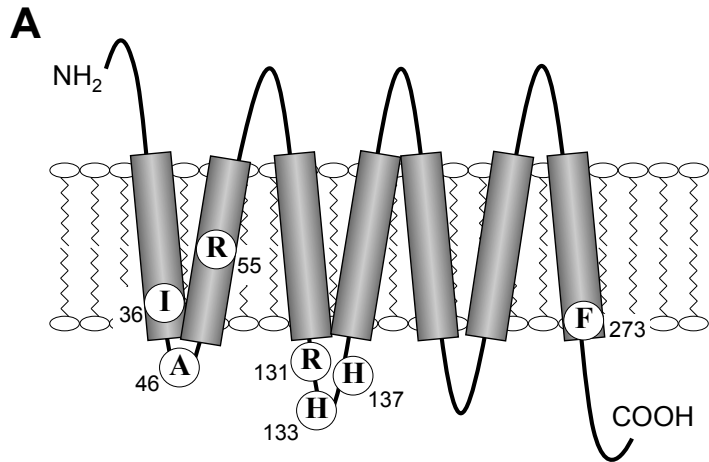


Figure_1.

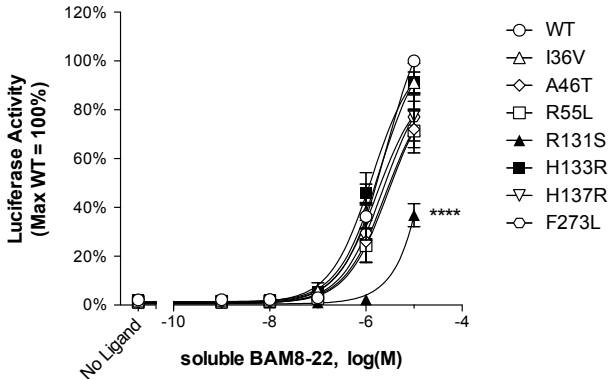
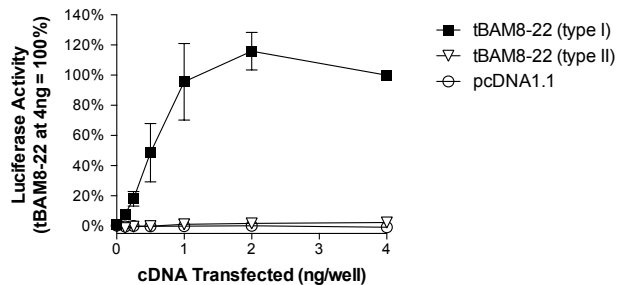
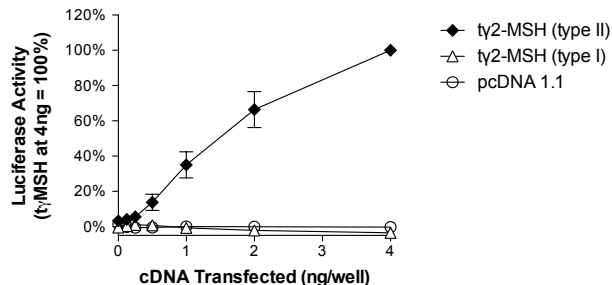
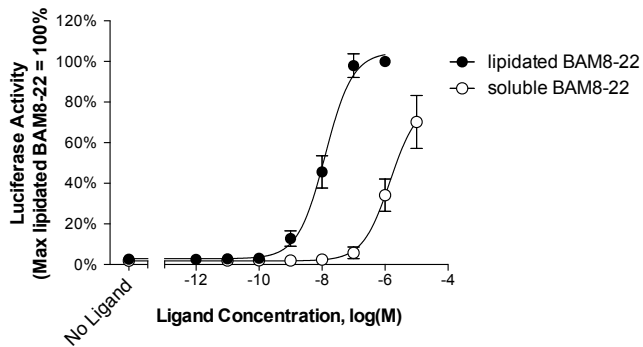
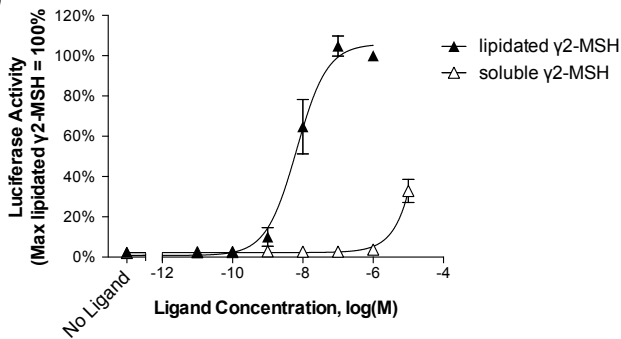
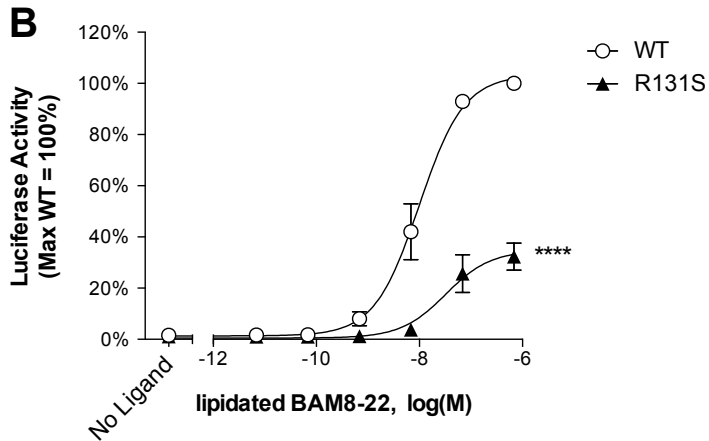
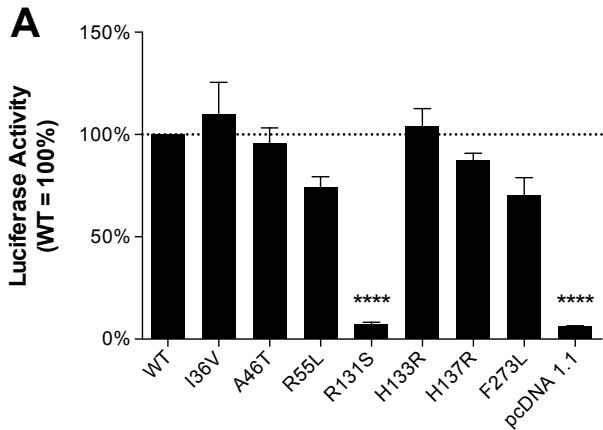
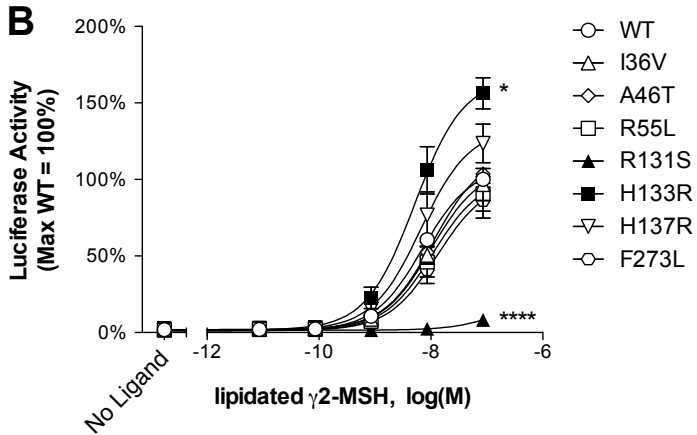
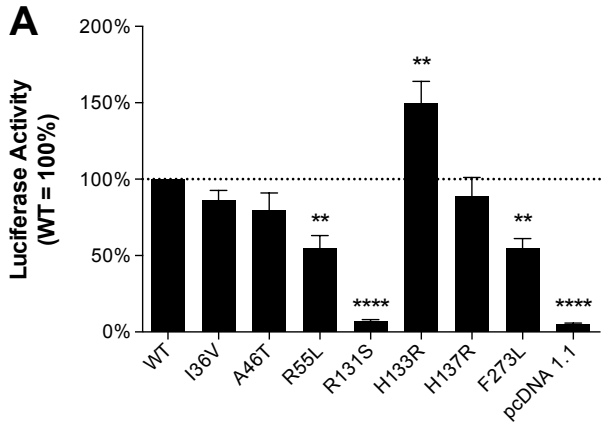


Figure 2

A**B****C****D****Figure_3**



Figure_4



Figure_5

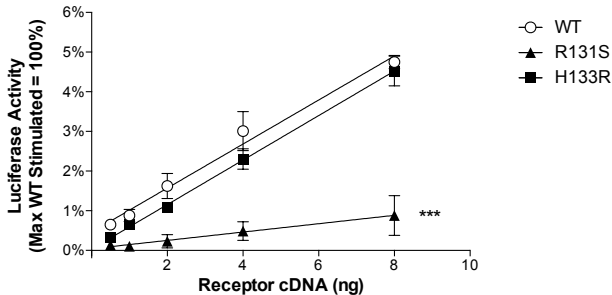
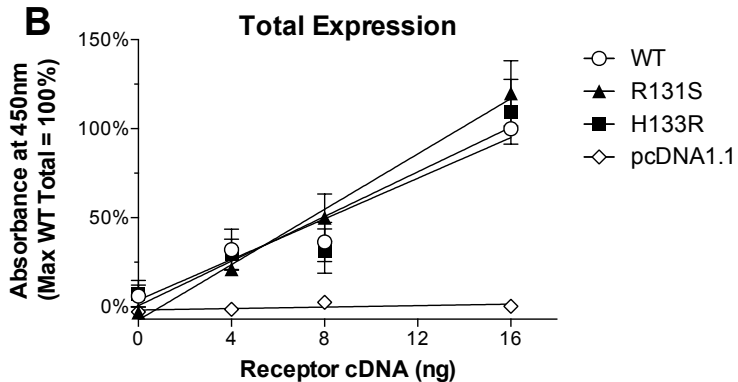
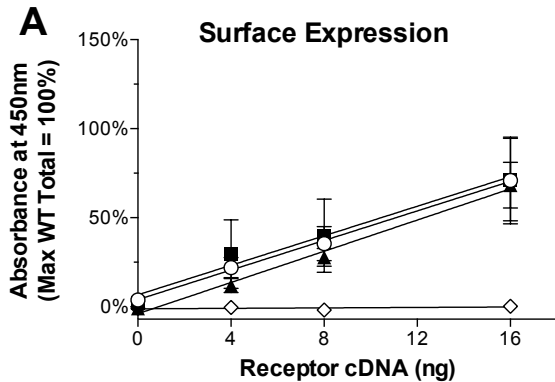


Figure 6



Figure_7